



HHS Public Access

Author manuscript

Carbohydr Polym. Author manuscript; available in PMC 2021 February 15.

Published in final edited form as:

Carbohydr Polym. 2020 February 15; 230: 115651. doi:10.1016/j.carbpol.2019.115651.

Accurate and sensitive quantitation of glucose and glucose phosphates derived from storage carbohydrates by mass spectrometry

Lyndsay E.A. Young¹, Corey O. Brizzee¹, Jessica K. A. Macedo¹, Robert D. Murphy¹, Christopher J. Contreras^{4,5}, Anna A. DePaoli-Roach^{4,5}, Peter J. Roach^{4,5}, Matthew S. Gentry^{1,3,5,6}, Ramon C. Sun^{2,6,*}

¹Department of Molecular and Cellular Biochemistry, University of Kentucky College of Medicine, Lexington, KY 40536, USA

²Department of Neuroscience, University of Kentucky College of Medicine, Lexington, KY 40536, USA

³University of Kentucky Epilepsy & Brain Metabolism Alliance, University of Kentucky College of Medicine, Lexington, KY 40536, USA

⁴Department of Biochemistry and Molecular Biology, Indiana University School of Medicine, Indianapolis, IN 46202

⁵Lafora Epilepsy Cure Initiative, University of Kentucky College of Medicine, Lexington, KY 40536, USA

⁶Markey Cancer Center, Lexington, KY 40536, USA

Abstract

The addition of phosphate groups into glycogen modulate its branching pattern and solubility which all impact its accessibility to glycogen interacting enzymes. As glycogen architecture modulates its metabolism, it is essential to accurately evaluate and quantify its phosphate content. Simultaneous direct quantitation of glucose and its phosphate esters requires an assay with high sensitivity and a robust dynamic range. Herein, we describe a highly-sensitive method for the accurate detection of both glycogen-derived glucose and glucose-phosphate esters utilizing gas-chromatography coupled mass spectrometry. Using this method, we observed higher glycogen levels in the liver compared to skeletal muscle, but skeletal muscle contained many more phosphate esters. Importantly, this method can detect femtomole levels of glucose and glucose

*To whom correspondence should be addressed: Ramon Sun: Department of Neuroscience BBSRB B179, University of Kentucky, Lexington, KY, 40536-0509 USA; ramon.sun@uky.edu; Tel. +1 (859)562-2298 Fax. +1 (859)323-5505.

Author contribution

Conceptualization, L.E.A.Y., and R.C.S.; Methodology, L.E.A.Y., C.J.C., M.S.G., and R.C.S.; Investigation, L.E.A.Y., C.O.B., J.K.A.M., R.D.M., and R.C.S.; Writing- Original Draft, L.E.A.Y., M.S.G., and R.C.S.; Writing- Review & Editing, L.E.A.Y., C.O.B., J.K.A.M., R.D.M., A.A.D., P.J.R., M.S.G., and R.C.S.; Funding Acquisition, M.S.G., and R.C.S.; Resources, A.A.D., P.J.R., M.S.G., and R.C.S.; Supervision, M.S.G., and R.C.S.

Publisher's Disclaimer: This is a PDF file of an unedited manuscript that has been accepted for publication. As a service to our customers we are providing this early version of the manuscript. The manuscript will undergo copyediting, typesetting, and review of the resulting proof before it is published in its final form. Please note that during the production process errors may be discovered which could affect the content, and all legal disclaimers that apply to the journal pertain.

phosphate esters within an extremely robust dynamic range with excellent accuracy and reproducibility. The method can also be easily adapted for the quantification of plant starch, amylopectin or other biopolymers.

Keywords

GCMS; glycogen; glucose; glucose phosphate esters; Lafora disease; laforin

1. Introduction

Glycogen is a branched polymer of glucose moieties that functions as an energy reserve in mammals. Glycogen is found in most tissues, including liver (Costill, Gollnick, Jansson, Saltin, & Stein, 1973; Frost, 2004), muscle (Hultman & Nilsson, 1971), kidney (Krebs, Bennett, De Gasquet, Gascoyne, & Yoshida, 1963), brain (Brown & Ransom, 2007), and white blood cells (Gibb & Stowell, 1949). The synthesis and breakdown of glycogen involves several enzymes and regulatory proteins (Peter J Roach, Skurat, & Harris, 2001). Glycogen is composed of glucose moieties joined by α -1,4-glycosidic linkages, formed by glycogen synthase, and branches occurring every 12-14 units via α -1,6-glycosidic branches, catalyzed by glycogen branching enzyme. This unique organization allows cells to store molecules of up to \approx 55,000 glucose units in a water-soluble form with high packing density for maximum storage (Peter J Roach, 2002). During glycogenolysis (glycogen breakdown), glycogen phosphorylase (GP) (Johnson, 1992) releases glucose-1-phosphate molecules to fuel a wide range of metabolic processes (Agius, 2015). Glycogen synthesis and degradation either consumes or produces free glucose-6-phosphate (G6P) and glucose 1-phosphate, respectively, key metabolites essential for energy production, lipid generation, and nucleotide biosynthesis important for cellular physiology.

Glycogen contains phosphate monoester groups covalently attached to the C2-, C3-, and C6-position of glucose hydroxyls (DePaoli-Roach et al., 2015; Nitschke et al., 2013; Peter J Roach, 2015; Tagliabracci et al., 2011). Glycogen-bound phosphate modulates glycogen architecture by affecting branching and chain length that define glycogen granular size, solubility, and its accessibility to glycogen interacting enzymes (Deng et al., 2015; Li, Powell Prudence, & Gilbert Robert, 2017; Powell et al., 2015; Worby, Gentry, & Dixon, 2006). Liver glycogen has an average chain length of 13 residues (Nitschke et al.; Peter J. Roach, Depaoli-Roach, Hurley, & Tagliabracci, 2012) and approximately 1 phosphate per 1,000-10,000 glucose residues (Nitschke et al.; Tagliabracci et al., 2011). These properties allow liver glycogen to maintain maximum solubility for rapid turn-over during periods of starvation. Muscle glycogen is architecturally distinct from liver glycogen. Muscle glycogen has higher levels of phosphate esters and altered branching pattern compared to liver glycogen. It is a fuel storage depot for the fight-or-flight response and does not contribute to the regulation of blood glucose (Raja, Bräu, Palmer, & Fournier, 2003; Tagliabracci et al., 2011). While the mechanism of phosphate incorporation into glycogen remains unresolved, glycogen phosphorylation is intimately linked with the biophysical properties and biological utilization of glycogen (A. Blennow & Engelsens, 2010; Nitschke et al., 2013; Silver, Kotting, & Moorhead, 2014; Sullivan et al., 2019). The importance of regulating glycogen

architecture and phosphorylation is highlighted in Lafora disease (LD). LD is an early onset neurodegenerative disease resulting from the accumulation of hyperphosphorylated, aberrant glycogen aggregates that drive disease pathogenesis in the form of myoclonic seizures, neuroinflammation, and premature death (Matthew S Gentry, Dixon, & Worby, 2009; Matthew S. Gentry, Guinovart, Minassian, Roach, & Serratosa, 2018; Nitschke, Ahonen, Nitschke, Mitra, & Minassian, 2018).

Glucose-2-phosphate (G2P), glucose-3-phosphate (G3P) and glucose-6-phosphate (G6P) are the hydrolyzed monomeric forms of glycogen. Although G2P, G3P and G6P are biochemically similar, G6P is a naturally occurring free metabolite that participates in glycolysis and the pentose phosphate pathway. G6P can be measured via spectrophotometric methods utilizing G6P dehydrogenase and NADP/NADPH conversion or a resorufin fluorescence assay (DePaoli-Roach et al., 2015; Zhu, Romero, & Petty, 2011). Conversely, no enzyme that utilizes G2P or G3P has been discovered, so the two cannot be distinguished by conventional biochemical enzymatic assays. Current technologies that can unambiguously distinguish G2P, G3P and G6P are 2D-nuclear magnetic resonance (NMR) and capillary electrophoresis (CE). 2DNMR is time consuming, requires a minimum of micrograms to milligrams of glycogen for accurate assignment, and it is challenging to adapt for routine laboratory analysis (Roden & Shulman, 1999). Currently, fluorescence-assisted capillary electrophoresis (FACE) is the gold standard to quantify C3 and C6 phosphorylation of glucose residues in starch (Verbeke, Penvenne, D'Hulst, Rolando, & Szydlowski, 2016). For FACE, starch is hydrolyzed and the glucose moieties are conjugated to 8-aminopyrene-1,3,6-trisulfonic acid (APTS). The APTS-conjugated glucose moieties can then be quantified using CE with accurate measurements as low as 1 glucose phosphate/100-1,000 glucose residues in plant starch. However, mammalian glycogen often contains much less glucose-bound phosphate, on the order of 10- to 100-fold less, which is below the dynamic range for CE. In addition, the presence of free APTS and inherent variation in retention time both add additional difficulties for batch processing, especially with low phosphate levels. Therefore, a higher-throughout, more accessible assay is needed that yields a more robust dynamic range with higher reproducibility and simultaneous quantitation of glucose, G2P, G3P, and G6P.

Herein, we introduce a workflow for the extraction and quantitation of glycogen and its phosphate esters. Glycogen was hydrolyzed to glucose, G2P, G3P, and G6P monomers and separated by gas-chromatography coupled to a highly sensitive mass spectrometry (GCMS) that can analyze a robust dynamic range and sensitivity for all three metabolites. With the addition of an auto-sampler, this GCMS-based method can profile up to 120 samples/day with accuracy, reliability, and reproducibility for routine interrogation of glucose moieties from mammalian glycogen and other glucose-based biopolymers.

2. Experimental Procedures

2.1. Materials

Analytical standards of D-glucose from Sigma Aldrich (Cas# 50-99-7), Glucose-2-phosphate synthesized by Christopher Contreras, Glucose-3-phosphate synthesized by Chiroblock, and D-Glucose-6-phosphate disodium salt, $C_6H_{11}Na_2O_9P \cdot xH_2O$, from Sigma

Aldrich (CAS #3671-99-6) were used throughout the study. Wild-type potato starch from Sigma Aldrich (CAS #9005-25-8) was purchased to test versatility of the method. *gwd*^{-/-} *Arabidopsis* starch was a generous gift from Drs. Sam Zeeman and Diana Santelia. Mice were housed in a climate-controlled environment with a 14/10-hour light/dark cycle (lights on at 0600 hours) with water and solid diet provided *ad libitum* throughout the study. The Institutional Animal Care and Use Committee at University of Kentucky has approved all of the animal procedures carried out in this study under PHS Assurance #A3336-01.

2.2. Chemical synthesis of Glucose-2-phosphate

Cyclic glucose-1,2 phosphate was synthesized using a method previously described by Zmudzka and Shugar (Zmudzka & Shugar, 1964). Briefly, glucose-1-phosphate (0.2g/ml), was converted to its free acid by cation exchange chromatography, neutralized immediately with pyridine and concentrated volume of approximately 10 ml in a vacuum centrifuge. 30 ml of pyridine and 3 g of dicyclohexylcarbodiimide was added, mixed and incubated at 0°C for 48 hours. Following removal of insoluble material, the barium salt of the glucose cyclic phosphate was precipitated using acetone by centrifugation for 5 minutes at 5,000 x g. The cyclic phosphate was washed in ethanol and acetone followed by acid hydrolysis to produce glucose-2-phosphate (De Clercq & Shugar, 1972; Piras, 1963).

2.3. Glycogen Purification

Mice were sacrificed by spinal dislocation, and liver and muscle were removed immediately post-mortem, and washed once with PBS, twice with diH₂O, blotted dry, and snap frozen in Liquid nitrogen. The frozen tissues were pulverized to 5 µm particles in liquid N₂ using a Freezer/Mill Cryogenic Grinder (SPEX SamplePrep). Twenty milligrams of each pulverized tissue were extracted in 50% methanol/chloroform (V/V 1:1) and separated into polar (aqueous layer), lipid (chloroform layer) and protein/DNA/glycogen (interfacial layer) fractions. Glycogen is further purified from protein/DNA using 1.5ml of ice cold 10% trichloroacetic acid. The glycogen fraction and polar fraction were dried by vacuum centrifuge at 10⁻³ mBar for hydrolysis and derivatization.

2.4. Glycogen and Starch Hydrolysis

Hydrolysis of glycogen and starch was performed by first resuspending the pellet in diH₂O followed by the addition equal parts 2N HCl. Samples were vortexed thoroughly and incubated at 95 °C for 2 hours. The reaction was quenched with 100% methanol with 40 µM L-norvaline (as an internal control). The sample was then incubated on ice for at least 30 minutes. The supernatant was collected by centrifugation at 15,000 rpm at 4°C for 10 minutes and subsequently dried by vacuum centrifuge at 10⁻³ mBar.

2.5. Sample Derivatization

Dried hydrolyzed glycogen samples were derivatized by the addition of 20mg/ml methoxyamine in pyridine and sequential addition of N-methyl-trimethylsilylation (MSTFA). Both steps were incubated for 60 minutes at 60 °C with thorough mixing in between addition of solvents. The mixture was then transferred to a v-shaped glass chromatography vial and analyzed by the GCMS.

2.6. GCMS Quantitation

Initial GCMS quantitation of the analytical standards, glycogen and starch are described previously from the Fiehn metabolomics GC method with the following modifications: the initial rate was held at 60 °C for 1 minute followed by 1-minute of run time, rising at 10 °C/minute to 325 °C and holding for 10 minutes followed by a run for 37.5 minutes (Fiehn et al., 2000; Kind et al., 2009). Adaptation of the Fiehn method is the following for rapid separation of Glucose-, G3P-, and G6P-6TMS;1MEOX: the initial rate was held at 60 °C for 1 minute followed by a 1 -minute run. Ramp 1: rising at a rate of 60 °C/minute reaching 220 °C and running for 3.67 minutes. Ramp 2: rising at 30 °C/minute reaching 270 °C and running for 5.33 minutes. Ramp 3: rising at 30 °C/minute to 325 °C, holding for 5 minutes and running for 12.2 minutes followed by a post run of 60 °C for 1 minute. The electron ionization was set to 70eV. Select ion monitoring mode was used for quantitative measurement. Ions used for the metabolites that represent glycogen are: glucose (319, 364), G3P, and G6P (315, 357, 387), and L-norvaline (174). Batch data processing was performed Masshunter software from Agilent. Glucose, G3P, and G6P were standardized to procedural control, norvaline, before quantitated using standard curve generated from known standards.

2.7. Statistics

Statistical analyses were carried out using GraphPad Prism. All numerical data are presented as mean \pm SD. Grouped analysis was performed using two-way ANOVA. Column analysis was performed using one-way ANOVA or t-test. A P-value less than 0.05 was considered statistically significant.

3. Results

3.1. Chemical derivatization of Glucose, G2P, G3P, and G6P

Previous work utilizing multiple tissues demonstrated the reliable and sensitive separation of free sugarphosphates after chemical derivatization for metabolomics applications (Fiehn, 2016). We hypothesized that this method could also separate G2P, G3P and G6P following hydrolysis of glycogen. Since G2P is not commercially available, we chemically synthesized G2P from G1P using a 2-step cyclic reaction with dicyclohexylcarbodiimide and barium salt (De Clercq & Shugar, 1972; Piras, 1963; Zmudzka & Shugar, 1964). The three glucose phosphate were subjected to a two-step derivatization procedure using analytical standards to convert them to volatile trimethylsilyl (TMS) derivatives that can be detected by a mass spectrometer (Quéro et al., 2014; Zarate et al., 2017). In the first step, the methoxylamination reaction replaces the oxygen atom of the alpha-carbonyl groups with methoxyamine (MEOX). Then silylation is performed in the second derivatization step using N-methyl-N-trimethylsilylation (MSTFA) to introduce trimethylsilyl groups to the remaining 6 carboxyl groups, replacing the acidic hydrogens (Fig. 1A-D). Methoxyamination generates both the syn- and ant-forms of MEOX at the alpha-carbonyl group, therefore resulting in the formation of a second much smaller peak with a small retention time shift that does not affect the quantification step (Fig. 2B). Trimethylsilylated metabolites are subjected to electron ionization (EI), where electrons fragment the molecules so that they can be registered by the mass spectrometer detector as molecular ions. The fragmentation pattern is consistent and reproducible across different GCMS platforms (Fig.

1A-D). In selected ion monitoring (SIM) mode, only specific fragment ions are detected by the mass spectrometer, significantly improving accuracy and sensitivity. Fragment ions (m/z) 319, 364 (glucose), 299, 357 and 387 (G2P, G3P, and G6P) were the major ions produced from EI-MS (Fig. 1A-D), and were used for the rest of the study in SIM mode to improve sensitivity of the GCMS.

3.2. Gas chromatography separation of Glucose, G2P, G3P, and G6P

G2P, G3P and G6P share similar chemical properties and specific detection has proven to be difficult. We hypothesized that the unique TMS derivatized form of G2P, G3P and G6P could be separated via gas chromatography (GC) given the appropriate temperature gradient. Each TMS derivative was analyzed separately using an adapted-Fiehn metabolomics GC method in full scan mode to confirm retention time (Fig. 2A) (Fiehn et al., 2000; Kind et al., 2009). Glucose-, G2P-, G3P-, and G6P-6TMS;1MEOX eluted at 17.6, 21.2, 20.1, and 21.9 minutes respectively (± 0.05 sec) and confirmed the utility of the GC to separate glucose and glucose phosphate esters (Fig. 2B). We identified the optimal separation temperature as 180-280° C with a ramp speed of 1° C/minute. These parameters were adapted and reduced the processing time to 12 minutes to provide a more rapid separation of the glucose moieties (Fig. 2C). We tested the ability of the rapid method to separate all three TMS derivatives with the new fast GCMS method using SIM mode. The retention times for glucose, G2P, G3P, and G6P were 6.25, 7.23, 7.11, and 7.39 minutes (± 0.05 sec), respectively (Fig. 2D). Thus, the rapid method yields a clear separation between glucose and each of the three phosphate esters.

3.3. Dynamic range of Glucose, G2P, G3P, and G6P

Mammalian glycogen contains 1 phosphate ester/1,000-10,000 glucose residues, approximately 10- to 100-fold lower glucose-bound phosphate than potato starch (DePaoli-Roach et al., 2015; Tagliabracci et al, 2011). To simultaneously detect glucose, G2P, G3P, and G6P monomers from glycogen, an assay with a robust and dynamic range is needed. Following the successful separation of TMS derivatized glucose moieties, we proceeded to determine the sensitivity and dynamic range for each molecule. Current GCMS models offer 10^6 dynamic range, which would be sufficient to measure glucose and phosphate esters simultaneously. We tested the limit of detection and dynamic range using the traditional 10:1 split mode of the GC inlet. In split mode, the limit of detection was 10 fmol for all three compounds with a dynamic range of 10 fmol to 1 μ mol (Fig. 3A-D). We did not test the range any lower or higher as it is either beyond the physiological range or potentially damaging to the ion source of the mass spectrometer. Cumulatively, these data confirm that GCMS analysis is extremely versatile for the separation of glucose, G2P, G3P, and G6P and it possesses a robust dynamic range that is well-suited for the analysis of a wide range of biopolymers.

3.4. Quantitation of glycogen and phosphate from mouse skeletal muscle and liver

Glycogen architecture gives rise to unique physiochemical properties that cause barriers to its own purification. The current method of glycogen purification from tissue uses 10% trichloroacetic acid (TCA) for low phosphate glycogen such as liver, and boiling the tissue in potassium hydroxide for muscle or other high phosphate containing glycogen molecules

(DePaoli-Roach et al., 2015). Both techniques require 0.1g-1g of tissue material due to low solubility of glycogen in each of the solvent, and they introduce variations in extraction efficiency and ambiguity in purity. In this study, we adapted a 2-step purification procedure that is highly efficient, and yields glycogen from as low as 20mg input from multiple tissues.

First, mouse liver and skeletal muscle were pulverized to 5 μm particles (subcellular volume) using a liquid nitrogen magnetic assisted tissue-grinding mill (Fig. 4A). After pulverization, 20mg of tissue was used for the glycogen purification method. Free polar metabolites and lipids were removed by the addition of polar and organic solvents, 50% Methanol:Chloroform (1:1). The insoluble glycogencontaining layer was collected and washed with 50% methanol and allowed to air dry. The glycogen was extracted with the addition of 10% trichloroacetic acid followed by vigorous mixing. The glycogencontaining TCA fraction was then separated from other insoluble material by centrifugation, and the glycogen was dried by vacuum centrifuge at 10^{-3} mBar, hydrolyzed to monomers by first resuspending in deionized H_2O followed by the addition of an equal part of 2N HCl and the reaction was carried out at 95°C for 2 hours. Hydrolysis was quenched with 100% methanol, 40 μM L-norvaline (as an internal control), and the sample was incubated on ice for 30 minutes. The supernatant was collected following a 10-minute 15,000 rpm spin at 4° C and dried by vacuum centrifuge at 10^{-3} mBar. The dried glucose moieties were derivatized by MEOX and MSTFA as described above, and then analyzed by GCMS (Fig. 4A). The polar fraction and the last wash were also analyzed as positive and negative controls (blank), respectively. The analysis found that liver glycogen contains 18 ± 3 μmol of glucose, 4 ± 1 nmol of G2P, 4 ± 1 nmol of G3P, and 5 ± 1 nmol of G6P per g of wet tissue weight (Fig. 4B-G). Muscle stores lower levels of glycogen (1 ± 0.12 μmol glucose/g of wet tissue weight), but contains higher levels of phosphate esters with 12 ± 1 nmol G2P and G6P per g of wet tissue weight, and strikingly G3P is the most abundant glucose phosphate ester in muscle with around 20 ± 1 nmol per g of wet tissue weight (Fig. 4B-G). These levels are in the ranges of previously published results and confirm previous findings that demonstrated higher phosphate content in muscle glycogen (Carroll, Longley, & Roe, 1956; DePaoli-Roach et al., 2015; Nitschke et al., 2013; Pederson et al., 2005; Stapleton et al., 2014; Tagliabracci et al., 2011; Vernia et al., 2011). Finally, we observed G6P in both polar fractions of muscle and liver extracts, but G2P and G3P were not detected in the fractions as expected.

While the mechanism of glycogen phosphorylation is unresolved, reversible starch phosphorylation is well-characterized and thought to be integral for starch metabolism (Andreas Blennow, 2015; Mahlow, Orzechowski, & Fettke, 2016; Pfister & Zeeman, 2016). Transitory starch is synthesized during the day and degraded at night, and reversible starch phosphorylation is necessary for efficient degradation. Glucan water dikinase (GWD) phosphorylates hydroxyls at the C6-position of glucose moieties on the outer surface of starch (Ritte et al., 2002). This phosphorylation event triggers phosphorylation at the C3-position by phosphoglucan water dikinase (PWD) (Baunsgaard et al., 2005; Kötting et al., 2005). These coordinated phosphorylation events allow amylases to more efficiently liberate glucose from starch until they reach the phosphate moieties. The glucan phosphatases starch excess 4 (SEX4) and like-sex four2 (LSF2) then liberate the phosphate so that the process

continues (M. Gentry & Vander Kooi, 2015; Santelia et al., 2011). Plants lacking GWD activity lack starch phosphorylation at the C6- and C3-position (Baunsgaard et al., 2005).

To test the versatility of this method, we performed a similar GCMS analysis on starch and glycogen. We analyzed wild-type (WT) starch from potato, starch from *Arabidopsis* leaves lacking glucan water dikinase (*gwd*^{-/-}), and liver glycogen to determine if this method can distinguish the difference between different phosphate levels. As predicted, the method detected the highest level of phosphate content in WT starch followed next by liver glycogen. The *gwd*^{-/-} *Arabidopsis* starch contained no detectable G2P, G3P, or G6P (Fig. 5). These data confirm the application of this novel GCMS-based method to quantify glucose-based polymers beyond mammalian glycogen and demonstrate that it can be used for the quantitation of plant starch.

4. Discussion

GCMS instruments are routinely used in analytical chemistry and known for their resolution, dynamic range, reproducibility, and durability. A new generation of autosampler-enabled GCMS units are designed to provide a workhorse-platform that offer unmatched consistency and performance for a wide range of analytical needs. Basic and clinical researchers have developed GCMS-based methods for profiling an impressive array of small metabolites to study perturbations in cellular metabolism (Garcia & Barbas, 2011; Lisec, Schauer, Kopka, Willmitzer, & Fernie, 2006) and to uncover disease biomarkers (Dunn et al., 2011). In this study, we adapted the GCMS analytical platform for the analysis of glycogen architecture. We employed a two-step derivatization process utilizing MEOX and MSTFA yielded derivatives that were more phase volatile and chemically stable forms of glucose, G2P, G3P, and G6P (-6TMS;1MEOX). This procedure has been shown previously to dramatically reduce the boiling point, improve the thermal stability, and enhance the chromatography separation of metabolites. We demonstrate the distinct separation of glucose, G2P, G3P, and G6P using a 12-minute chromatography method with a 10 fmol to 10 μ mol dynamic range. This method is extremely robust, medium-throughput (120 samples/day), and can be adapted for the characterization of plant starch and amylopectin.

Accurate quantitation of carbohydrate polymers and phosphate esters remains challenging due to their unique biochemical and biophysical properties. We developed a workflow to purify glycogen from only 20mg of mouse tissue and accurately quantified the glycogen-derived glucose and glucose phosphate esters using GCMS. Based on the dynamic range of GCMS, this method can be further adapted to utilize even less sample input, perhaps at the single cell level. We demonstrate an unambiguous measurement of glycogen-derived glucose, G2P, G3P, and G6P from muscle and liver. Our results align with previously published results, except with the higher levels of G3P detected by GCMS. This is not surprising as muscle glycogen varies with age (Cartee, 1994), sex (Ramamani, Aruldas, & Govindarajulu, 1999), and circadian rhythm (Takahashi et al., 2015). This new method utilizes less tissue to purify the glycogen and allows simultaneous quantification of glucose, G2P, G3P, and G6P. The application of this method is further demonstrated by the analysis of wild type potato starch, liver glycogen, and *gwd*^{-/-} starch (Ritte et al., 2006). This

analysis confirms previous results that *gwd*^{-/-} starch lacks phosphate and demonstrates the range in defining G6P between plant starch and liver glycogen.

This method will allow the robust analysis of glycogen polymers that accumulate in human glycogen storage diseases (GSD). The GSDs are a unique collection of monogenic diseases that share the accumulation of aberrant glycogen aggregates. While each GSD yields a glycogen-like aggregate, the exact architecture of the aggregate is unknown for many of the GSDs. Understanding the glycogen architecture would assist in defining the mechanism of disease pathology and facilitate with assessment of future treatment efficacy. Similarly, starch phosphorylation impacts multiple aspects of starch industrial processing. Starch is both a first-generation biofuel and industrial feedstock for paper, textiles, adhesives, and plastics. Phosphorylation is the only known natural modification of starch, and it directly influences starch hydration, crystallinity, freeze-thaw stability, viscosity, and transparency, which are all central to industrial applications (Santelia & Zeeman, 2011). This method would also allow rapid analysis of starch from multiple species and genotypes.

Acknowledgements:

We would like to thank Dr. Craig Vander Kooi and Gentry lab members for helpful discussion regarding the work.

Funding:

This study was supported by National Institute of Neurological Disorders and Stroke (R01 N070899-06, P01 NS097197-01), National Science Foundation (MCB-1817414), the University of Kentucky Center for Cancer and Metabolism, National Institute of General Medical Sciences COBRE program (P20 GM121327), American Cancer Society institutional research grant #16-182-28, and St Baldrick's Career Development Award, funding from the University of Kentucky Markey Cancer Center, and the University of Kentucky Epilepsy & Brain Metabolism Alliance. This research was also supported by funding from the University of Kentucky Markey Cancer Center, NIH National Center for Advancing Translational Sciences UL1TR001998, the Biostatistics and Bioinformatics Shared Resource Facility of the University of Kentucky Markey Cancer Center P30CA177558.

References:

- Agius L (2015). Role of glycogen phosphorylase in liver glycogen metabolism. *Molecular Aspects of Medicine*, 46, 34–45. [PubMed: 26519772]
- Baunsgaard L, Lütken H, Mikkelsen R, Glaring MA, Pham TT, & Blennow A (2005). A novel isoform of glucan, water dikinase phosphorylates pre-phosphorylated α -glucans and is involved in starch degradation in *Arabidopsis*. *The Plant Journal*, 41(4), 595–605. [PubMed: 15686522]
- Blennow A (2015). Phosphorylation of the starch granule In *Starch* (pp. 399–424): Springer
- Blennow A, & Engelsen SB (2010). Helix-breaking news: fighting crystalline starch energy deposits in the cell. *Trends Plant Sci*, 15(4), 236–240. [PubMed: 20149714]
- Brown AM, & Ransom BR (2007). Astrocyte glycogen and brain energy metabolism. *Glia*, 55(12), 1263–1271. [PubMed: 17659525]
- Carroll NV, Longley RW, & Roe JH (1956). The determination of glycogen in liver and muscle by use of anthrone reagent. *J Biol Chem*, 220(2), 583–593. [PubMed: 13331917]
- Cartee GD (1994). Influence of age on skeletal muscle glucose transport and glycogen metabolism. *Medicine and science in sports and exercise*, 26(5), 577–585. [PubMed: 8007805]
- Costill DL, Gollnick PD, Jansson ED, Saltin B, & Stein EM (1973). Glycogen Depletion Pattern in Human Muscle Fibres During Distance Running. *Acta Physiologica Scandinavica*, 89(3), 374–383. [PubMed: 4767239]
- De Clercq E, & Shugar D (1972). Antiviral activity of polynucleotides: role of the 2'-hydroxyl and a pyrimidine 5-methyl. *FEBS Letters*, 24(1), 137–140. [PubMed: 4343812]

- Deng B, Sullivan MA, Wu AC, Li J, Chen C, & Gilbert RG (2015). The Mechanism for Stopping Chain and Total-Molecule Growth in Complex Branched Polymers, Exemplified by Glycogen. *Biomacromolecules*, 16(6), 1870–1872. [PubMed: 25933040]
- DePaoli-Roach AA, Contreras CJ, Segvich DM, Heiss C, Ishihara M, Azadi P, & Roach PJ (2015). Glycogen Phosphomonoester Distribution in Mouse Models of the Progressive Myoclonic Epilepsy, Lafora Disease. *The Journal of Biological Chemistry*, 290(2), 841–850. [PubMed: 25416783]
- Dunn WB, Broadhurst D, Begley P, Zelena E, Francis-McIntyre S, Anderson N, ... The Human Serum Metabolome. C. (2011). Procedures for large-scale metabolic profiling of serum and plasma using gas chromatography and liquid chromatography coupled to mass spectrometry. *Nature Protocols*, 6, 1060. [PubMed: 21720319]
- Fiehn O (2016). Metabolomics by Gas Chromatography-Mass Spectrometry: Combined Targeted and Untargeted Profiling. *Current protocols in molecular biology*, 114, 30.34.31–30.34.32. [PubMed: 27038389]
- Fiehn O, Kopka J, Dörmann P, Altmann T, Trethewey RN, & Willmitzer L (2000). Metabolite profiling for plant functional genomics. *Nature Biotechnology*, 18(11), 1157.
- Frost LD (2004). Glucose Assays Revisited: Experimental determination of the glucose concentration in honey. *The Chemical Educator*, 9(4), 239–241.
- Garcia A, & Barbas C (2011). Gas chromatography-mass spectrometry (GC-MS)-based metabolomics In *Metabolic Profiling* (pp. 191–204): Springer
- Gentry M, & Vander Kooi C (2015). Thermophilic phosphatases and methods for processing starch using the same. Google Patents.
- Gentry MS, Dixon JE, & Worby CA (2009). Lafora disease: insights into neurodegeneration from plant metabolism. *Trends in biochemical sciences*, 34(12), 628–639. [PubMed: 19818631]
- Gentry MS, Guinovart JJ, Minassian BA, Roach PJ, & Serratos JM (2018). Lafora disease offers a unique window into neuronal glycogen metabolism. *Journal of Biological Chemistry*, 293(19), 7117–7125. [PubMed: 29483193]
- Gibb RP, & Stowell RE (1949). Glycogen in human blood cells. *Blood*, 4(5), 569–579. [PubMed: 18120777]
- Hultman E, & Nilsson LH (1971). Liver Glycogen in Man. Effect of Different Diets and Muscular Exercise. In Pernow B & Saltin B (Eds.), *Muscle Metabolism During Exercise: Proceedings of a Karolinska Institutet Symposium held in Stockholm, Sweden, September 6–9, 1970* Honorary guest: E Hohwü Christensen (pp. 143–151). Boston, MA: Springer US
- Johnson LN (1992). Glycogen phosphorylase: control by phosphorylation and allosteric effectors. *The FASEB Journal*, 6(6), 2274–2282. [PubMed: 1544539]
- Kind T, Wohlgemuth G, Lee DY, Lu Y, Palazoglu M, Shahbaz S, & Fiehn O (2009). FiehnLib: mass spectral and retention index libraries for metabolomics based on quadrupole and time-of-flight gas chromatography/mass spectrometry. *Analytical chemistry*, 81(24), 10038–10048. [PubMed: 19928838]
- Kötting O, Pusch K, Tiessen A, Geigenberger P, Steup M, & Ritte G (2005). Identification of a novel enzyme required for starch metabolism in *Arabidopsis* leaves. The phosphoglucan, water dikinase. *Plant physiology*, 137(1), 242–252. [PubMed: 15618411]
- Krebs HA, Bennett DAH, De Gasquet P, Gascoyne T, & Yoshida T (1963). Renal gluconeogenesis. The effect of diet on the gluconeogenic capacity of rat-kidney-cortex slices. *Biochemical Journal*, 86(1), 22–27. [PubMed: 14035641]
- Li C, Powell Prudence O, & Gilbert Robert G (2017). Recent progress toward understanding the role of starch biosynthetic enzymes in the cereal endosperm. *Amylase* (Vol. 1, p. 59).
- Lisec J, Schauer N, Kopka J, Willmitzer L, & Fernie AR (2006). Gas chromatography mass spectrometry-based metabolite profiling in plants. *Nature Protocols*, 1(1), 387. [PubMed: 17406261]
- Mahlow S, Orzechowski S, & Fettke J (2016). Starch phosphorylation: insights and perspectives. *Cellular and molecular life sciences*, 73(14), 2753–2764. [PubMed: 27147464]
- Nitschke F, Ahonen SJ, Nitschke S, Mitra S, & Minassian BA (2018). Lafora disease—from pathogenesis to treatment strategies. *Nature Reviews Neurology*, 1.

- Nitschke F, Wang P, Schmieder P, Girard J-M, Awrey Donald E., Wang T, ... Minassian Berge A. (2013). Hyperphosphorylation of Glucosyl C6 Carbons and Altered Structure of Glycogen in the Neurodegenerative Epilepsy Lafora Disease. *Cell Metabolism*, 17(5), 756–767. [PubMed: 23663739]
- Pederson BA, Schroeder JM, Parker GE, Smith MW, DePaoli-Roach AA, & Roach PJ (2005). Glucose metabolism in mice lacking muscle glycogen synthase. *Diabetes*, 54(12), 3466–3473. [PubMed: 16306363]
- Pfister B, & Zeeman SC (2016). Formation of starch in plant cells. *Cellular and molecular life sciences*, 73(14), 2781–2807. [PubMed: 27166931]
- Piras R (1963). SYNTHESIS OF SOME ALDOSE 2-PHOSPHATES. *Archives of Biochemistry and Biophysics*, 103,291–292. [PubMed: 14084595]
- Powell PO, Sullivan MA, Sheehy JJ, Schulz BL, Warren FJ, & Gilbert RG (2015). Acid hydrolysis and molecular density of phytoglycogen and liver glycogen helps understand the bonding in glycogen alpha (composite) particles. *PLoS One*, 10(3), e0121337. [PubMed: 25799321]
- Quéro A, Jousse C, Lequart-Pillon M, Gontier E, Guillot X, Courtois B, ... Pau-Roblot C (2014). Improved stability of TMS derivatives for the robust quantification of plant polar metabolites by gas chromatography–mass spectrometry. *Journal of Chromatography B*, 970, 36–43.
- Raja G, Bräu L, Palmer TN, & Fournier PA (2003). Repeated bouts of high-intensity exercise and muscle glycogen sparing in the rat. *Journal of experimental biology*, 206(13), 2159–2166. [PubMed: 12771165]
- Ramamani A, Aruldas M, & Govindarajulu P (1999). Differential response of rat skeletal muscle glycogen metabolism to testosterone and estradiol. *Canadian journal of physiology and pharmacology*, 77(4), 300–304. [PubMed: 10535679]
- Ritte G, Heydenreich M, Mahlow S, Haebel S, Kötting O, & Steup M (2006). Phosphorylation of C6- and C3- positions of glucosyl residues in starch is catalysed by distinct dikinases. *FEBS Letters*, 580(20), 4872–4876. [PubMed: 16914145]
- Ritte G, Lloyd JR, Eckermann N, Rottmann A, Kossmann J, & Steup M (2002). The starch-related R1 protein is an α -glucan, water dikinase. *Proceedings of the National Academy of Sciences*, 99(10), 7166–7171.
- Roach PJ (2002). Glycogen and its metabolism. *Current molecular medicine*, 2(2), 101–120. [PubMed: 11949930]
- Roach PJ (2015). Glycogen phosphorylation and Lafora disease. *Molecular Aspects of Medicine*, 46, 78–84. [PubMed: 26278984]
- Roach PJ, Depaoli-Roach AA, Hurley TD, & Tagliabracci VS (2012). Glycogen and its metabolism: some new developments and old themes. *The Biochemical journal*, 441(3), 763–787. [PubMed: 22248338]
- Roach PJ, Skurat AV, & Harris RA (2001). Regulation of glycogen metabolism. *The endocrine pancreas and regulation of metabolism*, 2, 609–647.
- Roden M, M, & Shulman GIM., PhD, (1999). Applications of NMR spectroscopy to study muscle glycogen metabolism in man. *Annual review of medicine*, 50(1), 277–290.
- Santelia D, K-tting O, Seung D, Schubert M, Thalmann M, Bischof S, ... Gentry MS (2011). The phosphoglucan phosphatase like sex Four2 dephosphorylates starch at the C3-position in *Arabidopsis*. *The Plant Cell*, 23(11), 4096–4111. [PubMed: 22100529]
- Santelia D, & Zeeman SC (2011). Progress in *Arabidopsis* starch research and potential biotechnological applications. *Current Opinion in Biotechnology*, 22(2), 271–280. [PubMed: 21185717]
- Silver DM, Kötting O, & Moorhead GB (2014). Phosphoglucan phosphatase function sheds light on starch degradation. *Trends Plant Sci*.
- Stapleton DI, Lau X, Flores M, Trieu J, Gehrig SM, Chee A, ... Koopman R (2014). Dysfunctional muscle and liver glycogen metabolism in mdx dystrophic mice. *PLoS One*, 9(3), e91514. [PubMed: 24626262]
- Sullivan MA, Nitschke S, Skwara EP, Wang P, Zhao X, Pan XS, ... Lee JP (2019). Skeletal Muscle Glycogen Chain Length Correlates with Insolubility in Mouse Models of Polyglucosan-Associated Neurodegenerative Diseases. *Cell Reports*, 27(5), 1334–1344. e1336. [PubMed: 31042462]

- Tagliabracci Vincent S., Heiss C, Karthik C, Contreras Christopher J., Glushka J, Ishihara M, ... Roach Peter J. (2011). Phosphate Incorporation during Glycogen Synthesis and Lafora Disease. *Cell Metabolism*, 13(3), 274–282. [PubMed: 21356517]
- Takahashi H, Kamei A, Osawa T, Kawahara T, Takizawa O, & Maruyama K (2015). 13C MRS reveals a small diurnal variation in the glycogen content of human thigh muscle. *NMR in Biomedicine*, 28(6), 650–655. [PubMed: 25881007]
- Verbeke J, Penverne C, D'Hulst C, Rolando C, & Szydlowski N (2016). Rapid and sensitive quantification of C3-and C6-phosphoesters in starch by fluorescence-assisted capillary electrophoresis. *Carbohydrate polymers*, 152, 784–791. [PubMed: 27516330]
- Vernia S, Heredia M, Criado O, Rodriguez de Cordoba S, Garcia-Roves PM, Cansell C, ... Ferre P (2011). Laforin, a dual specificity phosphatase involved in Lafora disease, regulates insulin response and whole-body energy balance in mice. *Human Molecular Genetics*, 20(13), 2571–2584. [PubMed: 21493628]
- Worby CA, Gentry MS, & Dixon JE (2006). Laforin, a dual specificity phosphatase that dephosphorylates complex carbohydrates. *Journal of Biological Chemistry*, 281(41), 30412–30418. [PubMed: 16901901]
- Zarate E, Boyle V, Rupprecht U, Green S, Villas-Boas S, Baker P, & Pinu F (2017). Fully automated trimethylsilyl (TMS) derivatisation protocol for metabolite profiling by GC-MS. *Metabolites*, 7(1), 1.
- Zhu A, Romero R, & Petty HR (2011). An enzymatic colorimetric assay for glucose-6-phosphate. *Analytical Biochemistry*, 419(2), 266–270. [PubMed: 21925475]
- Zmudzka B, & Shugar D (1964). PREPARATION+ CHEMICAL+ ENZYMIC PROPERTIES OF CYCLIC PHOSPHATES OF D-GLUCOPYRANOSE+ SYNTHESIS OF DERIVATIVES OF N-(D-GLUCOPYRANOSYL) PYRIDINE. *Acta Biochimica Polonica*, 11(4), 509–&.

Highlights:

- Simultaneous quantitation of glucose and glucose phosphate esters in glycogen
- This assay provides robust dynamic range with excellent accuracy and reproducibility
- Quantitation of glucose-2-phosphate with in-house synthesized standard
- This assay can be adapted for plant starch, amylopectin or other biopolymers

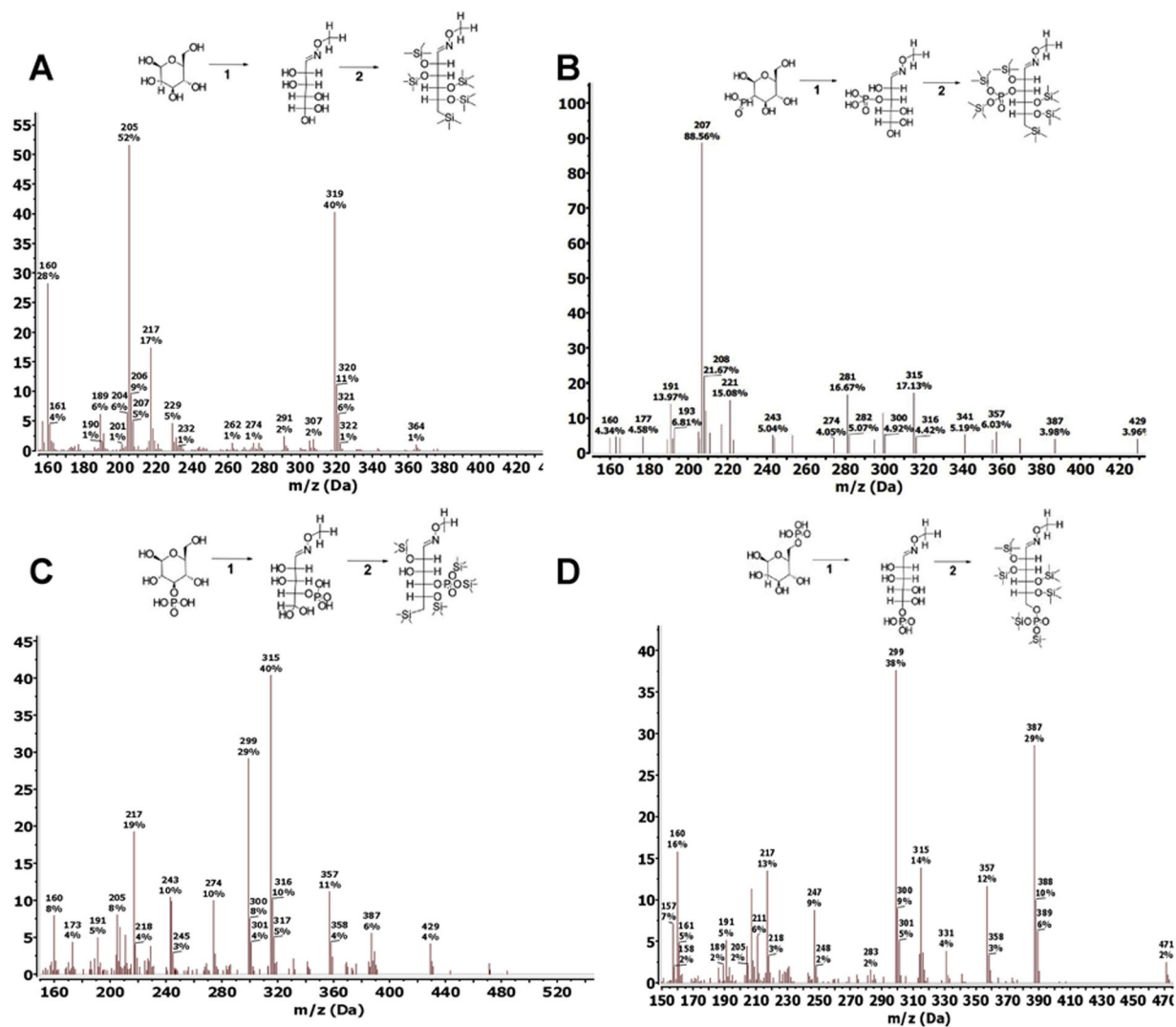


Fig. 1. Derivatization and fragmentation pattern of glucose, G2P, G3P, G6P.

Trimethylsilylation of analytical grade standards of glucose (A), G2P (B), G3P (C), and G6P (D) (–6TMS;1MEOX). Two μ moles of each standard were derivatized with 20mg/ml MEOX in pyridine for 1-hour (reaction 1), followed by silylation by MSTFA for 1-hour (reaction 2). Both reaction steps took place in a 60° C dry heat block. Fragmentation pattern for each silylated standard was obtained on a single quadrupole mass spectrometer with an electron ionization (EI) energy of 70 eV, mass range of 30-650 AMU, and 1.47 scan/s.

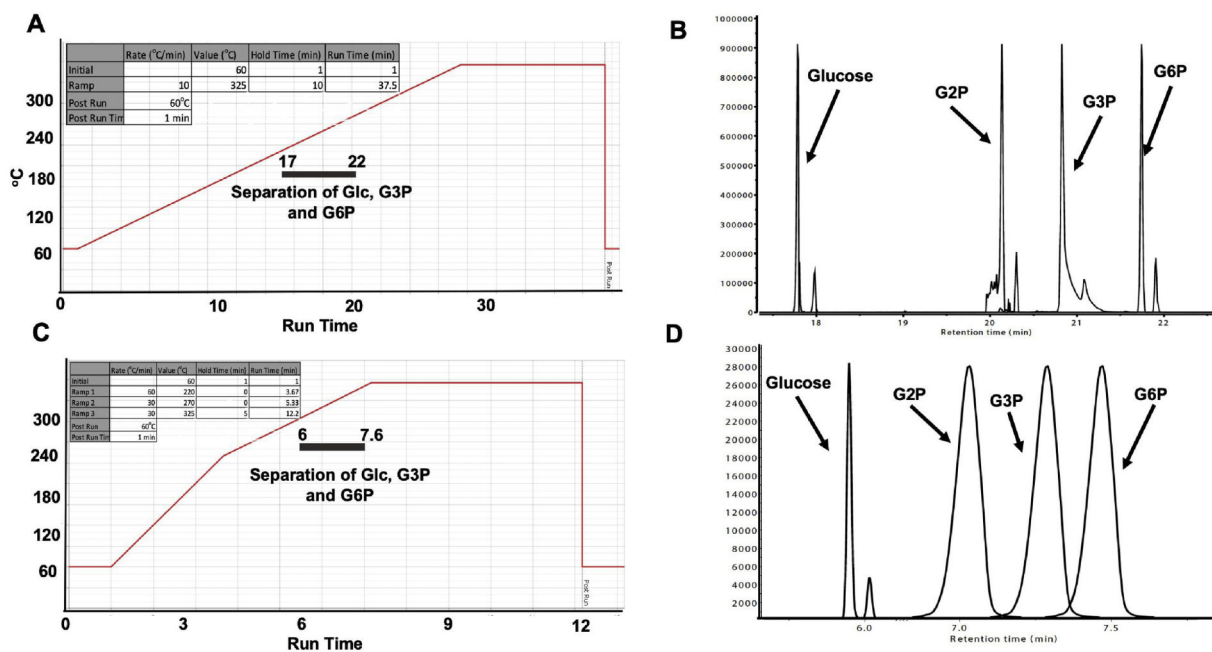


Fig. 2. Standard and rapid gas chromatography separation of glucose, G2P, G3P, G6P.

(A) Temperature gradient for standard separation of glucose, G3P, and G6P: Initial temperature was 60° C, held for 1 minute, rising at 10° C/minute to 325° C, held for 10 minutes. Total run time: 37.5 minutes. Grey bar indicates window of separation.

(B) Stacked chromatography spectra for silylated glucose, G2P, G3P, and G6P using the temperature setting in (A). Twenty nmoles of each silylated standard were injected into the GC column.

(C) Temperature gradient setting for rapid separation of glucose, G3P, and G6P: initial temperature was 60° C, held for 1 minute, rising at 60° C/minute to 220° C, continued rising at 30° C/minute to 270° C, and finished rising at 30° C/minute to 325° C, held for 5 minutes. Total run time: 12.2 minutes. Grey bar indicates window of separation.

(D) Stacked chromatography spectra for silylated glucose, G2P, G3P, and G6P combined into one sample using the temperature setting in (C). Two nmoles of each silylated standard were injected into the GC column.

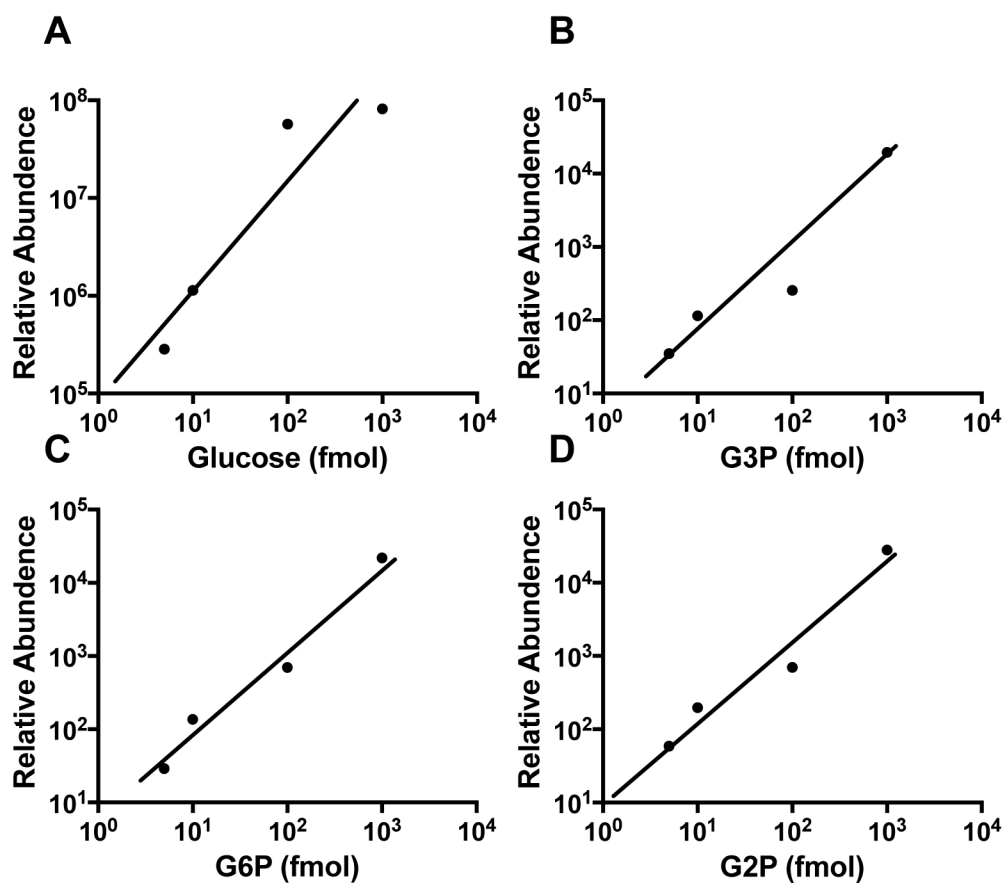


Fig. 3. Dynamic range of GCMS analysis of glucose, G3P, and G6P.

Silylated glucose (A), G3P (B), G6P (C), and G2P (D) standards at multiple concentrations were injected into the GC using split mode with a ratio of 10:1.

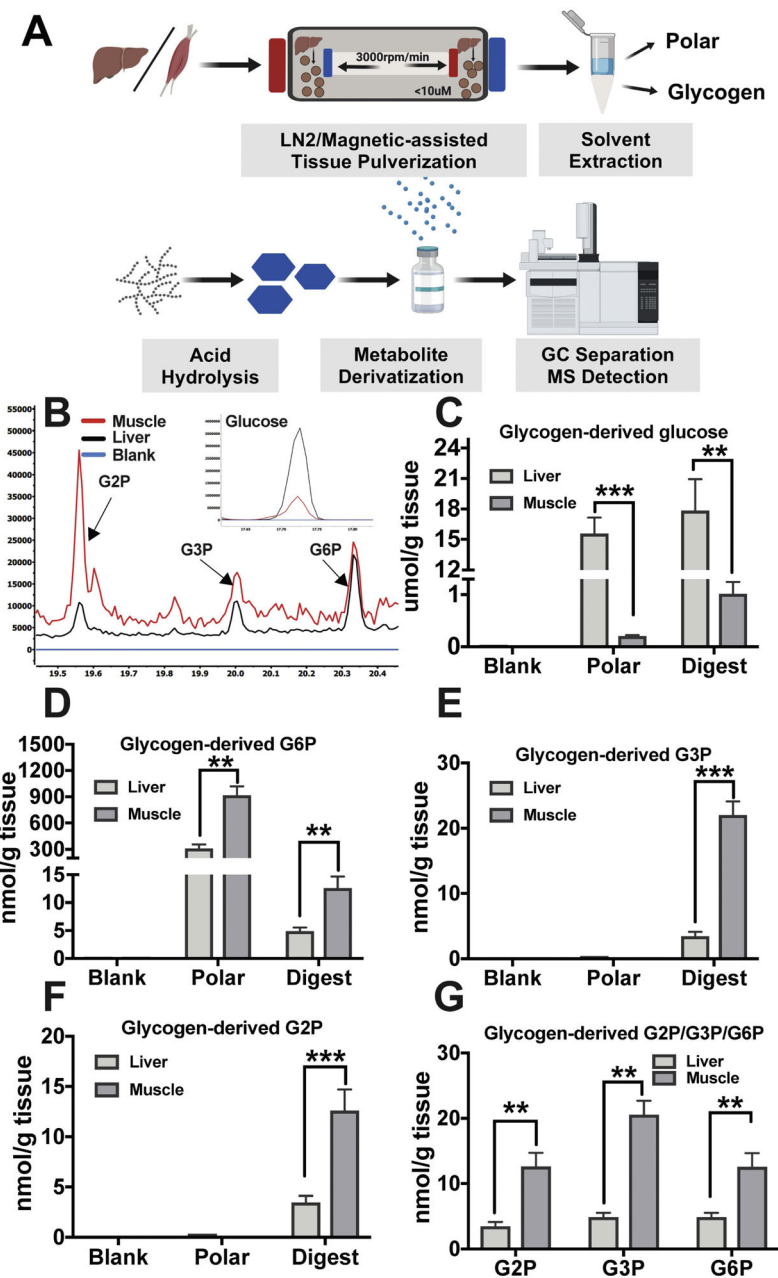


Figure 4: Extraction and GCMS analysis of liver and muscle glycogen

(A) Schematics of glycogen extraction: mouse liver or skeletal muscle were milled to 10 μm particles by liquid N₂ Freezer/Mill Cryogenics Grinder magnetic assisted tissue-grinding mill, followed by polar and organic solvent removal of free polar metabolites and lipids. Glycogen was then extracted by 10% TCA. Isolated glycogen was hydrolyzed to monomers by mild hydrolysis, derivatized by MEOX and MSTFA, and analyzed by GCMS (B). Quantitation of liver or muscle derived glucose (C), G6P (D), G3P (E), G2P (F) the third wash of tissue pellet is served as blank, and free polar metabolite fraction serves as negative control for G3P and G2P and a positive control for G6P. (F) Muscle contains higher G2P,

G3P and G6P than liver when standardized to tissue weight. Data shown in (C-G) are from three experiments and are shown as mean \pm SEM.

* p 0.05, ** p 0.01, *** p 0.001; two-tailed t -test.

Author Manuscript

Author Manuscript

Author Manuscript

Author Manuscript

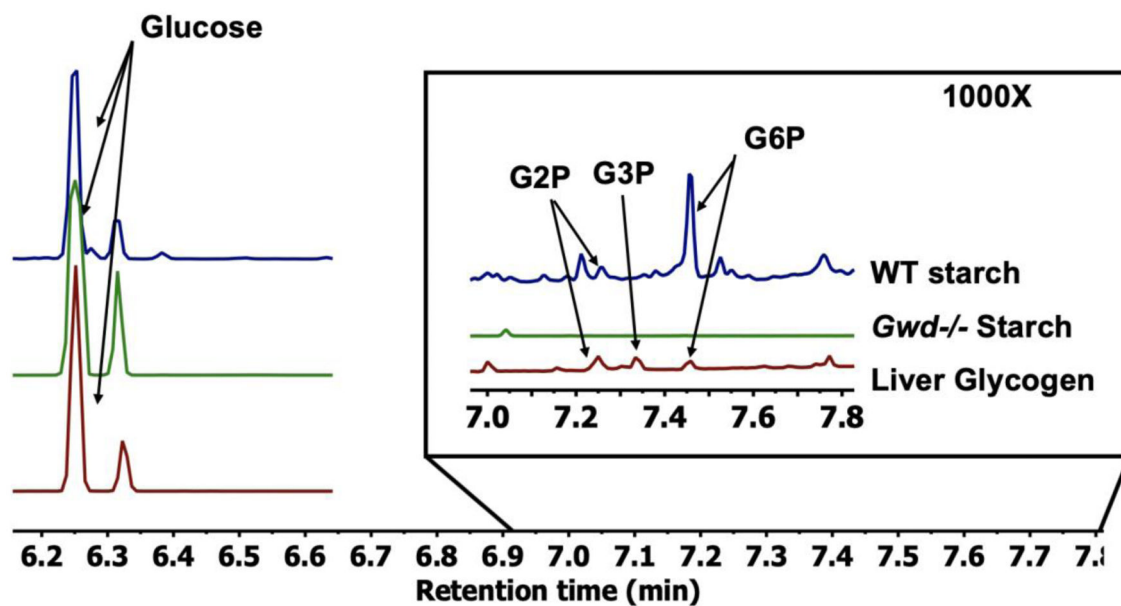


Fig. 5. Comparison between plant starch and mammalian liver glycogen. Stacked spectra overlay between WT potato starch, *gwd*^{-/-} *Arabidopsis* starch, and mammalian liver glycogen to demonstrate versatility of the approach. All three samples were standardized to total glucose. The region between 7-7.8 minutes demonstrates that WT plant starch contains 10-fold higher phosphate than liver glycogen, while no detectable phosphate was observed in the *gwd*^{-/-} *Arabidopsis* starch.